



# Evolutionary dynamics of plastomes within *Arisaema* (Araceae)

Shook Ling Low<sup>1</sup> · Sven Landrein<sup>2</sup>

Received: 13 January 2025 / Accepted: 9 March 2025  
© The Author(s) under exclusive licence to Archana Sharma Foundation of Calcutta 2025

## Abstract

*Arisaema*, the third largest genus in the family Araceae, exhibited remarkable morphological diversity and wide biogeographic distribution. However, its plastome evolution remains insufficiently explored. In this study, we analysed the complete chloroplast genomes of 13 *Arisaema* taxa spanning nine taxonomic sections, including a newly assembled plastome of *A. prazeri* from southwestern China. The plastomes exhibited a conserved quadripartite structure with no major structural rearrangements, though variations such as indels, repeats sequences, and IR expansion/contraction were observed. Sliding window and repeat structure analyses identified regions of high nucleotide diversity, particularly in the SSC and IR regions, suggesting potential mutation hotspots. Phylogenomic analyses provided enhanced resolution of interspecific relationships, notably repositioning *A. nepenthoides* as a sister lineage to all other sampled taxa. Despite extensive morphological diversification, plastome structure remains relatively stable across the genus, indicating the plastome evolution may be decoupled from morphological variation. Further exploration of nuclear and mitochondrial genomes is recommended to clarify the evolutionary mechanisms underlying *Arisaema* diversification and adaptation.

**Keywords** East Asia · Plastome evolution · Nucleotide diversity · Repeat structure

## Introduction

The genus *Arisaema* Mart., is one of the largest and most recently diversified lineages within the family Araceae, comprising approximately 180–207 species (Flora of China; Kew checklist of selected families). Characterized by remarkable morphological diversity, *Arisaema* has a broad biogeographic distribution, with over 95% of its species occurring

across temperate Asia, particularly in biodiversity hotspots such as India, China, and Japan [18]. The genus also extends into tropical regions, including Indochina and Sundaland, as well as part of North America and East Africa [20, 35, 36]. These species inhabit a wide range of ecosystems, from tropical and semi-evergreen forests to high-altitude grasslands, occurring from sea level up to 3700 m [32]. Like other members of the subfamily Aroideae, such as *Typhonium*, *Arum*, and *Amorphophallus*; *Arisaema* exhibits a dormancy phase, with only its underground tuber remaining viable during seasonal shifts [9, 30].

The infrageneric classification of *Arisaema* is based primarily on morphological traits, grouping species into 15 sections, further supported by phylogenetic analyses using four plastid regions (3'*trnL-trnF*, *rpl20-5'rps12*, *psbB-psbH* and *rpoC2-rps2*): sect. *Anomala*, sect. *Arisaema*, sect. *Attenuata*, sect. *Clavata*, sect. *Decipientia*, sect. *Dochafa*, sect. *Flagellarisaema*, sect. *Franchetiana*, sect. *Nepenthoidea*, sect. *Odorata*, sect. *Pistillata*, sect. *Sinarisaema*, sect. *Tenuipistillata*, sect. *Tortuosa*, and sect. *Frimbriata* [31, 38]. Despite this classification framework, plastome-based studies on *Arisaema* remain limited, with only about 5% of species having published plastome data, including *A. franchetianum*, *A. ringens*, and *A. erubescens* [6, 21, 47].

Corresponding Editor: Umesh C. Lavania; Reviewers: Arun Kumar Pandey, Mareike Roeder.

**Significant Statement:** This study enhances understanding of *Arisaema* plastome evolution by analyzing 13 taxa across nine taxonomic sections. Despite extensive morphological diversity, plastome structure remains stable, suggesting evolutionary decoupling and interspecific relationships. Findings highlight mutation hotspots and call for further nuclear and mitochondrial genome exploration.

✉ Shook Ling Low  
shookling.low@ibot.cas.cz

<sup>1</sup> Institute of Botany, Czech Academy of Sciences, 25243 Průhonice, Czechia

<sup>2</sup> Kadoorie Farm and Botanic Garden Corporation, Lam Kam Road, Tai Po, New Territories, Hong Kong S.A.R., China

This underrepresentation has hindered comprehensive assessments of plastome structure, evolution, and mutation dynamics within the genus.

In angiosperms, plastomes typically range from 120 to 180 kb and contain approximately 130 genes, organized into a quadripartite structure consisting of large single-copy (LSC), small single-copy (SSC), and two inverted repeats (IRs) [40]. Although plastome structure is largely conserved, structural variations such as inversions [7], translocations [26, 45], gene losses [16, 19], IR absences [8, 27], and other rearrangements [16] have been documented across different angiosperm lineages. In *Arisaema*, which began diversifying approximately 24 million years ago in the late Oligocene [37], the extent of plastome structural variation remain largely unexplored. To address this knowledge gap, we presents a de novo assembly of the plastome of *A. prazeri*, collected from karst outcrops in southwestern China, and compare it with twelve previously published *Arisaema* plastomes from different taxonomic sections. By investigating plastome structural variation and mutational dynamics, this study aims to enhance our understanding of plastome evolution in *Arisaema* and its potential links to the genus's evolutionary history.

## Material and methods

### Taxa sampling

*Arisaema prazeri* is distributed across karst landscapes in tropical southern to southwestern Yunnan, northern Myanmar, and Thailand [31]. Due to its small population size and ongoing deforestation in the area, only one specimen was collected from a karst outcrop located in Pao Zhu Qing (Xishuangbanna prefecture, Mengla county, Meng Xing town, China; Fig. 1). A voucher specimen has been deposited in the herbarium of Xishuangbanna Tropical Botanical Garden (HITBC).

### DNA isolation and illumina sequencing

Genomic DNA was extracted from *A. prazeri* using the standard Cetyl Trimethyl Ammonium Bromide (CTAB) protocol. High-quality DNA was quantified and outsourced to the Beijing Genomic Institute (BGI, Shenzhen) for sequencing. At BGI, a 5G raw data library was prepared, with DNA fragments sized between 300 and 350 bp. Sequencing was conducted on an Illumina HiSeq X 10 platform (Illumina Inc. USA). Details regarding library preparation and sequencing protocols are provided in Low et al. [30].

## Plastome assembly and annotation

Sequencing of *A. prazeri* yielded 5G of 150 bp single-end reads, generating 60,962,408 reads (approximately 9,106,476,796 bases). Adapter sequences and short fragments were removed using fastQC [3], and reads with an average Phred score of  $\geq 20$  were retained, resulting in 95.85% high quality reads.

In addition, Sequence Read Archive (SRA) data for *A. franchetianum*, and *A. heterophyllum* were downloaded from the National Center for Biotechnology (NCBI). Raw reads for *A. prazeri* from Thailand and *Pinellia ternata* were obtained from Low et al. [30]. High-quality paired-end reads were assembled using GetOrganelle ver.1.7.6.1 [23], with SPAdes [4]. Contigs were mapped using Bowtie2 [29]. For *A. heterophyllum*, a 3915 bp fragment was missing from the AT-rich region of the assembled plastome; therefore, the complete plastome sequence from Genbank was used instead (Table 1). The same approach was applied to species lacking SRA data, including *A. erubescens*, *A. ringens*, *A. bockii*, and *A. nepenthoides* (Table 1). The assembled plastome sequences were annotated using GeSeq on the Chlorobox platform [44], and the annotated *A. prazeri* plastome was deposited in NCBI under accession number OP644316.

## Phylogenetic analyses

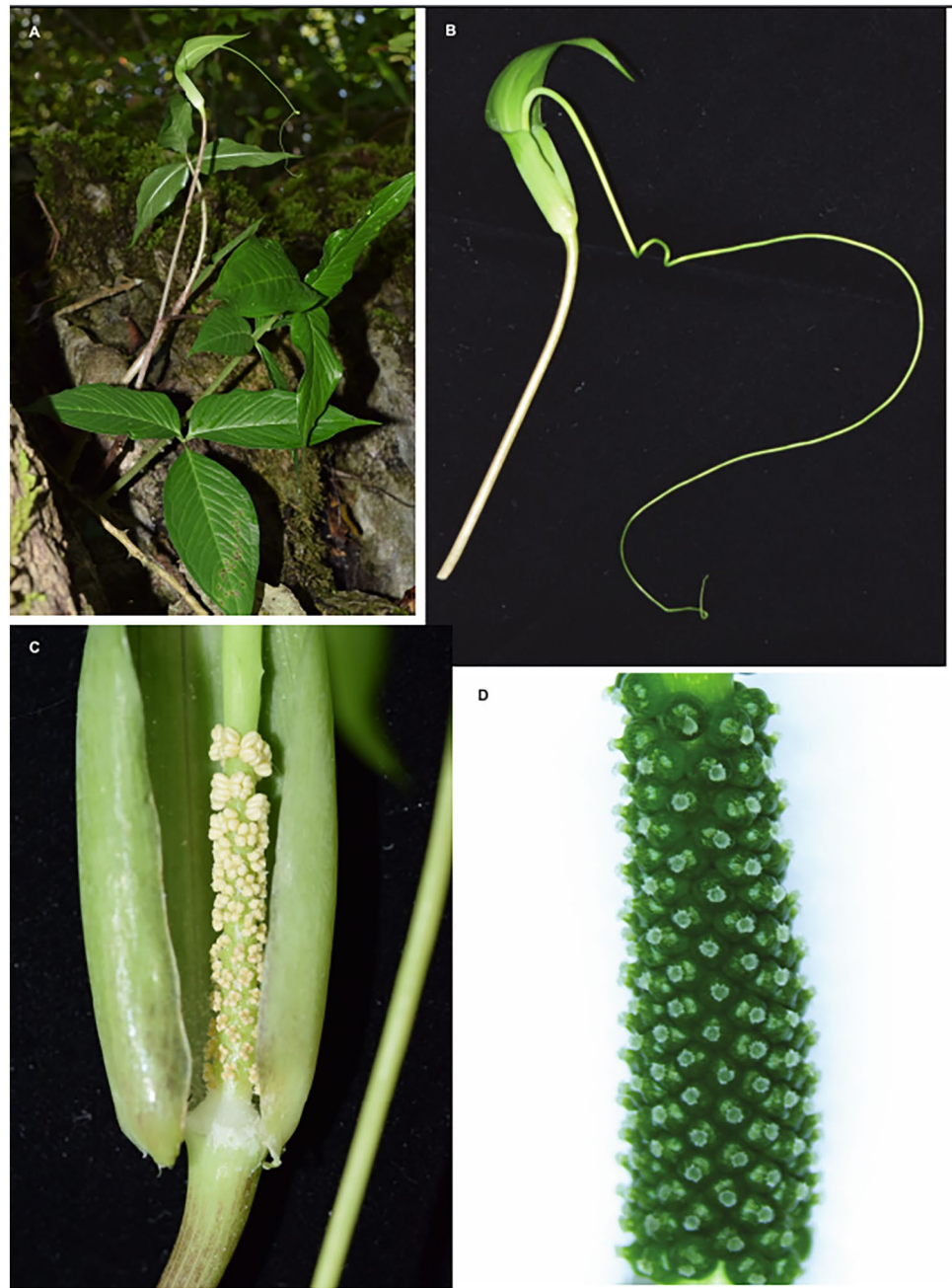
Phylogenetic reconstructions included Eleven species, comprising thirteen *Arisaema* plastomes representing nine of the fifteen recognized sections within the genus (Table 1). The analyzed taxa included *A. erubescens* (sect. Sinarisaema), *A. heterophyllum* (sect. Flagellarisaema), *A. bockii*, *A. ringens*, *A. amurense* (sect. Pistillata), *A. nepenthoides* (sect. Nepenthoidea), *A. franchetianum* (sect. Franchetiana), *A. flavum* (sect. Frimbiata), *A. decipiens* (sect. Decipientia), and *A. triphyllum* (sect. Pedatisecta). *Arisaema prazeri* belongs to sect. Odorata. To prevent over-weighting of IR regions, the IRa region was excluded (Low et al., in prep.).

Plastome sequences were concatenated and aligned using MAFFT-7.453 [24]. Phylogenetic relationships were inferred using IQtree2 with a Maximum Likelihood (ML) approach and 1000 bootstrap replicates [34]. Given that *Pinellia* is the sister genera to *Arisaema* [37], *P. ternata* [30] was used as the outgroup. The resulting tree topology was visualized using FigTree v1.4.3 (<http://tree.bio.ed.ac.uk/software/figtree/>).

## Plastome structures analysis

To assess plastome structural variation, we examined the contraction and expansion of IR regions and their boundaries with the single-copy (SC) regions. Gene distribution at the junctions of the SSC, LSC, IRa, and IRb regions were

**Fig. 1** Natural habitat and morphology of *Arisaema prazeri*. **A.** Karst habitat, **B.** Inflorescence, **C.** Staminate flowers with pollen extrusion, **D.** Pistillate flowers collected from YinChangShan



analysed using IRplus, an extension of IRscope available at <https://irscope.shinyapps.io/IRplus/> [2, 12]. This tool facilitated the identification of size variations and boundary shifts, providing insights into pseudogenization events.

To explore plastome rearrangements and inversions across *Arisaema* species, we used the progressive Mauve algorithm [10] within Geneious (<https://www.geneious.com>). Annotated plastome alignments were used to generate Locally Collinear Blocks (LCBs), representing homologous regions conserved across genomes. The default LCB weight was set to 3X the minimum match seed size, ensuring

reliable homology detection. Genome rearrangements and LCBs were visualized in the Mauve alignment viewer, and mapped onto the ML phylogenetic tree of *Arisaema* to correlate structural variations with evolutionary relationships.

### Sequence divergence analysis

To assess interspecific variation, a schematic representation of sequence divergence across twelve *Arisaema* plastomes was generated using mVISTA in Shuffle-LAGAN mode [17], with *P. ternata* as the reference. Gene annotations, including contig

**Table 1** Summary statistics of plastome feature across 13 *Arisaema* taxa

Taxa	Accession Number	Section	Plastome size (bp)/ GC content (%)	LSC size (bp)	IR size	SSC size (bp)	Number of annotated genes
<i>A. prazeri</i> - China	This study	Odorata	167,954/ 35.2	93,086	26,271	22,326	152
<i>A. prazeri</i> - Thailand	MT884869	Odorata	170,935/ 34.6	95,078	26,414	23,029	152
<i>A. erubescens</i>	MT676834	Sinarisaema	167,607 / 35.3	93,664	26,191	21,561	150
<i>A. heterophyllum</i>	MZ424448	Flagellarisaema	170,610 / 34.5	95,485	26,260	22,605	153
<i>A. heterophyllum</i>	ON060885	Flagellarisaema	170,554/ 34.5	95,436	26,260	22,598	155
<i>A. bockii</i>	MZ380241	Pistillata	175,537/ 33.6	97,874	27,159	23,345	152
<i>A. nepenthoides</i>	MW338731	Nepenthoidea	166,390 / 35.4	95,965	23,728	22,584	153
<i>A. franchetianum</i>	SRR8655277	Franchetiana	169,480 / 34.9	94,743	26,391	21,955	152
<i>A. flavum</i>	MZ568767	Frimbiata	167,582/35.3	96,705	24,329	22,208	150
<i>A. decipiens</i>	ON360980	Decipientia	167,792/35.0	93,691	26,182	21,737	152
<i>A. triphyllum</i>	SRR18716441	Pedatisecta	171,245/34.4	95,356	26,825	22,219	155
<i>A. ringens</i>	MK111107	Pistillata	160,792/ 36.5	88,915	25,312	21,253	153
<i>A. amurense</i>	OR789627	Pistillata	171,454/34.4	95,953	26,512	22,477	152

positions and orientations, were provided as generic feature format (gff) files to enhance alignment accuracy. The resulting “peaks and valleys” plot illustrated sequence conservation and divergence across taxa.

Nucleotide polymorphism (Pi) was quantified using DnaSP v6.12.03, with a sliding window of 600 bp and a step size of 200 bp [39]. This analysis allowed for precise identification of highly polymorphic plastome regions, facilitating comparative sequence diversity assessments.

### Repeat sequence characterization

Long repetitive DNA sequences within the plastomes were identified using REPuter, which detects forward, reverse, complementary, and palindromic repeats. The thresholds for repeat identification was set at a minimum length of 30 bp with a Hamming distance of 3 and a similarity index greater than 90% [28].

Simple sequence repeats (SSRs) were identified using the MISA tool (<https://webblast.ipk-gatersleben.de/misa/>). Detection parameters were set for mono-, di-, tri-, tetra-, penta-, and hexanucleotide repeats, with thresholds of 10, 5, 4, 3, 3, and 3 repeat units, respectively [5, 43].

## Results

### Chloroplast genomes

The fully assembled chloroplast genome of *A. prazeri* from Xishuangbanna spans 167,954 bp. The MAFFT alignment of *A. prazeri*, together with 12 additional *Arisaema* taxa, and *P. ternata* resulted in 194,151 bases, with 74.4% sequence identity among taxa.

All chloroplast genomes exhibited a typical quadripartite structure, with sizes ranging from 160,792 bp in *A. ringens* to 175,537 bp in *A. bockii*. The large single copy (LSC) region spans 88,915 bp in *A. ringens* to 97,874 bp in *A. bockii*, the small single copy (SSC) region ranging from 21,253 bp in *A. ringens* to 23,345 bp in *A. bockii*, and a pair of inverted repeat IR<sub>A</sub> and IR<sub>B</sub> that vary from 23,728 bp in *A. nepenthoides* to 27,159 bp in *A. bockii* (Fig. 2, Table 1). GC content varied from 33.6% in *A. bockii* to 36.5% in *A. ringens*. The plastomes encoded between 150 and 155 unique genes (Table 1; Supplemental Table 1).

### Phylogenomic analyses

The ML tree was well-supported (Bootstrap Probability, BP = 100%, Fig. 2), reflecting robust phylogenetic relationships. A notable exception was *A. franchetianum*, which formed a sister clade with *A. erubescens* and *A. flavum* but received moderate support (BP = 93%).

### Plastome structure

Gene distribution at inverted repeat (IR) and single-copy (SC) junctions varied among *Arisaema* species. In most species, the SSC/IR borders contained the *ndhF* gene, except in *A. ringens* and *A. nepenthoides*, where it was adjacent to *ycf2*. The *ycf1* gene was consistently positioned across species, except in *A. ringens*, *A. decipiens* and *A. nepenthoides*. Notably, *A. prazeri* exhibited an inversion of *ndhF* and *ycf1*. The LSC/IR<sub>B</sub> (J<sub>LB</sub>) junction was typically located between *rps19* and *rpl2*, except in *A. nepenthoides*, where it was within *rpl2*. Additionally, *A. decipiens* contained a

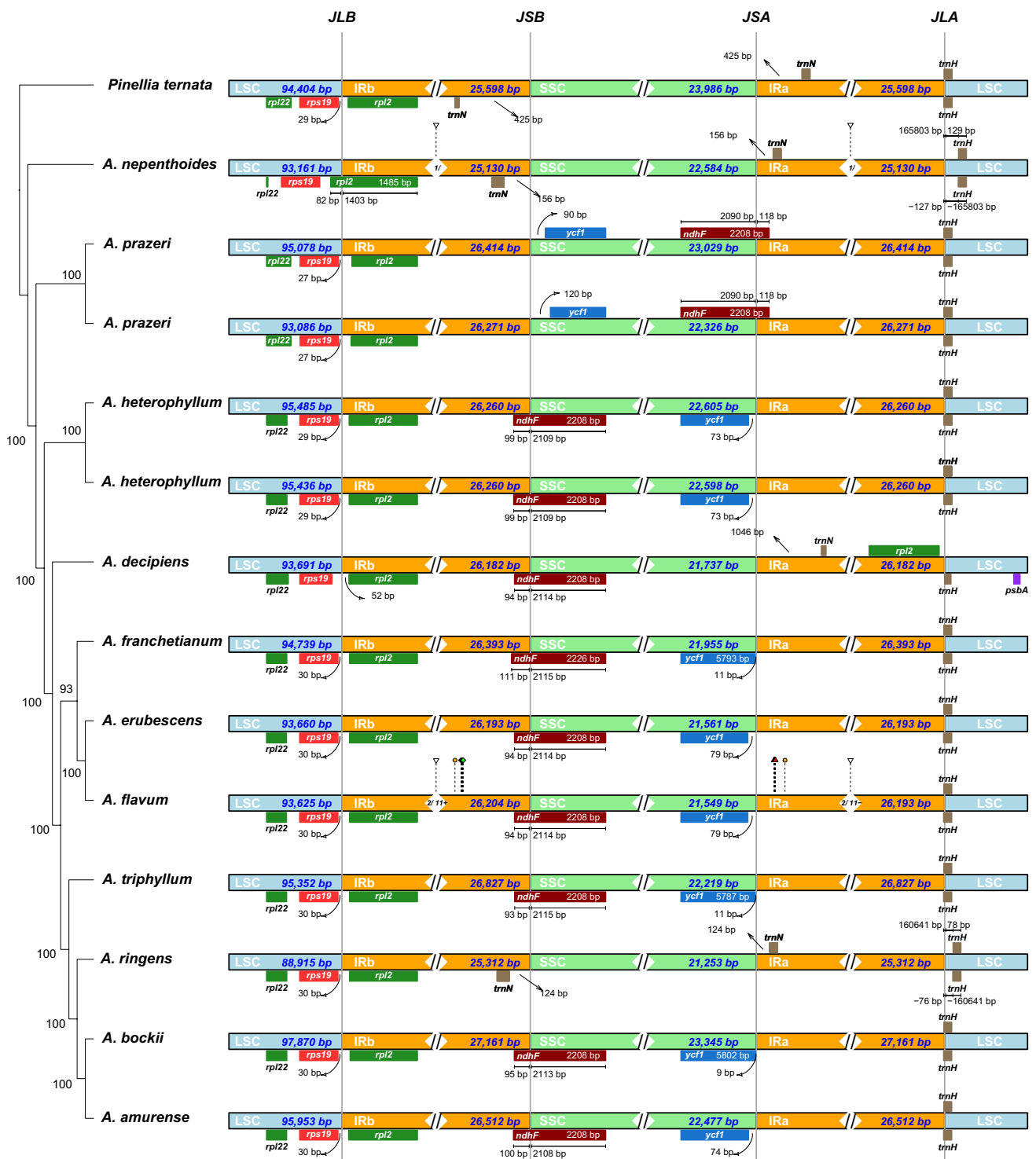


**Fig. 2** Maximum likelihood (ML) phylogenetic tree of 13 *Arisaema* taxa, mapped with plastome structures

duplicated *rpl2* gene near the LSC/IR<sub>A</sub> (J<sub>LA</sub>) junction. The LSC/IR<sub>A</sub> (J<sub>LA</sub>) junction was generally located between *rpl2* and *trnH*, except in *A. nepenthoides*. While most genes remained within their respective SC or IR regions, *A. heterophyllum* displayed an extension of the *trnH* gene into the

IR<sub>A</sub> region by a single base pair (Fig. 2). The plastome of *A. nepenthoides* exhibited distinct characteristics, with both SSC/IR borders adjacent to *ycf2*; while the LSC/IR borders were defined by *rpl2* and *rpl23*, respectively (Fig. 2).

Alignment via Mauve, using *P. ternata* as a reference, revealed eight syntenic blocks across taxa (Fig. 3). The largest locally collinear blocks (LCBs), represented in green, were found in the LSC and IRb regions, while cyan and dark blue blocks corresponded to sequences in the SSC and IR regions. These blocks were homologous across taxa, but appeared inverted in *A. prazeri*. While overlap of these three blocks was common across quadripartite

structures, it was absent in *A. triphyllum*. Additionally, five smaller syntenic blocks, spanning only a few hundred base pairs, were present in some taxa.

mVISTA analysis revealed that the LSC region exhibited the highest divergence among *Arisaema* species, followed by the SSC region; while IR regions were highly conserved. However, *A. ringens* showed divergence in two untranslated regions [UTRs] within the IR regions (Fig. 4, Supplemental

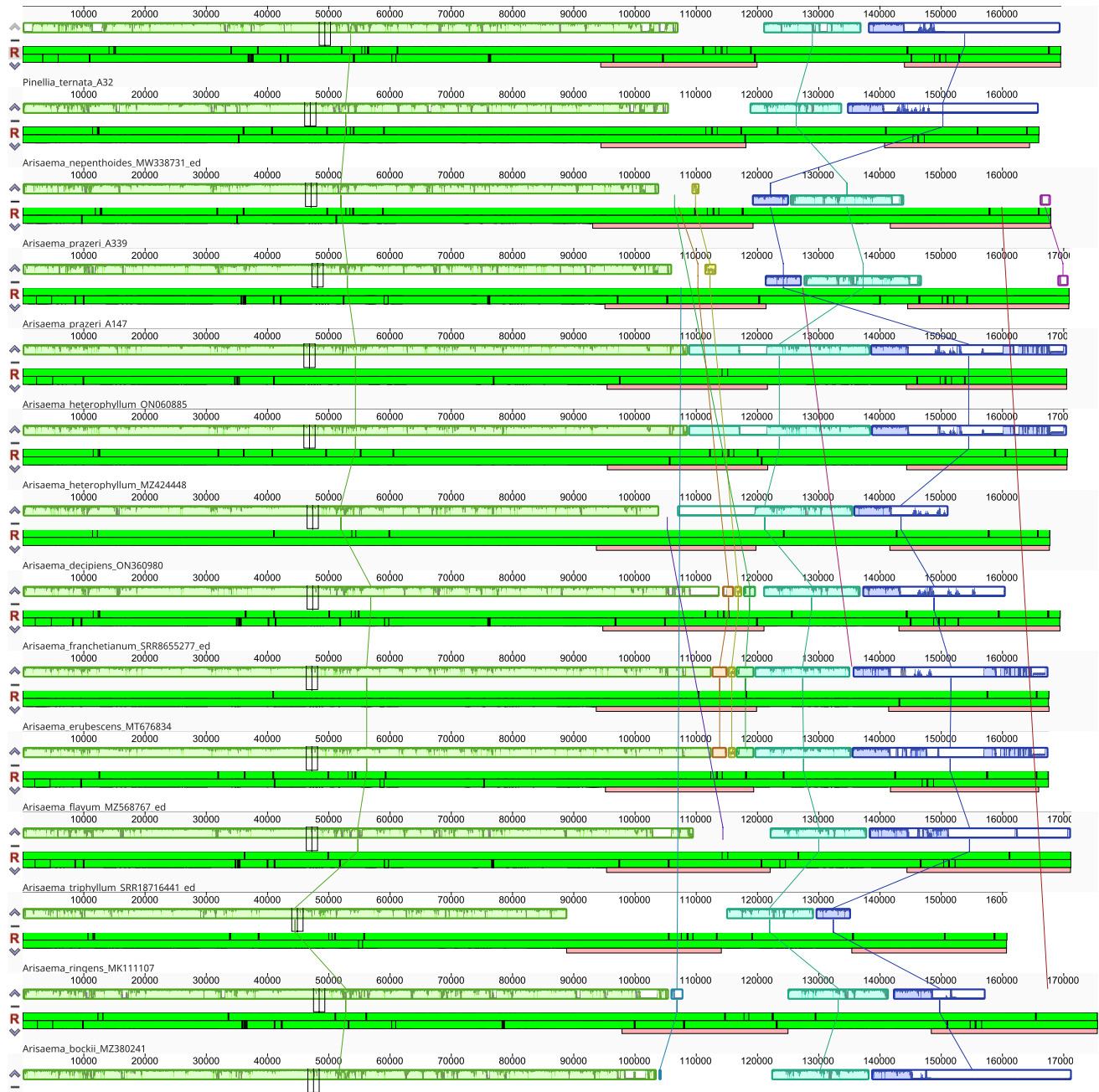


**Fig. 3** Gene rearrangement analysis of 13 *Arisaema* taxa using Mauve alignment. Colored blocks indicate homologous regions across genomes, with each color distinguishing a different locally collinear block (LCB)

Fig. 1). Conserved non-coding sequences (NCS) displayed greater variability than coding regions.

### Nucleotide diversity analysis

DnaSP analysis of 191,462 base pairs (153,593 non-gap sites) identified 7588 polymorphic sites and 7863 mutations, indicating high genetic diversity (Fig. 5, Supplemental Table 2). Each of the 13 analyzed sequences was unique, resulting in a haplotype diversity (Hd) of 1.000 with minimal variance, highlighting substantial genetic differentiation. The overall nucleotide diversity ( $\pi$ ) was 0.01059, indicating moderate genetic variability, while the average number of nucleotide differences ( $k$ ) between sequences was 1,625.897, further emphasizing genetic diversity within the genus.

Mutation rate estimates (Theta,  $\theta$ ) provided additional insights. Theta-W ( $\theta_W$ ), based on segregating sites, was 0.01592 per site, while Theta from total mutations was 0.01650 per site. Using a finite sites model, Theta from  $\pi$  was 0.01074, aligning closely with observed nucleotide diversity. These estimates suggest that mutations significantly contribute to genetic variation in *Arisaema*.

A sliding window analysis revealed regional variation in nucleotide diversity across the chloroplast genome. The SSC region, particularly positions 134,562–136,886, which including *trnH-GUG*, *trnN-GUU*, and *ndhF*, exhibited the highest diversity ( $\pi = 0.06887$ ). Another peak was observed in the *ycf1* region (positions 157,589 to 159,021) with  $\pi = 0.03882$ , suggesting potential adaptive evolution. Unexpectedly high diversity was found in the IRa region around *rrn23* gene (positions 168,137 to 169,834;  $\pi = 0.05333$ ), a typically conserved region, indicating unique evolutionary dynamics. Moderate diversity was detected in the LSC region, particularly positions 66,459–67,847 (*trnH-GUG* and *accD*;  $\pi = 0.05265$ ). Regions associated with *psaC* and *ycf1* in the SSC (positions 145,193–157,588) displayed moderate diversity, suggestive of ongoing mutation and genetic drift. Conversely, some regions showed very low nucleotide diversity, suggesting strong conservation. For instance, towards the end of the analyzed sequences (positions 186,721–191,462), the diversity values were minimal, with  $\pi$  values as low as 0.00026 (positions 188,745–189,359), indicating these regions are functionally important and evolutionarily conserved.

### Repeat structure analysis

The REPuter tool identified four classes of long sequences repeats—forward, reverse, complementary, and palindromic sequences across *Arisaema* plastome. Forward sequences were most frequent in *A. amurense*, *A. bockii*, *A. decipiens*, *A. erubescens*, *A. franchetianum*, *A. heterophyllum* (two accessions), *A. nepenthoides*, *A. prazeri* (two accessions),

*A. ringens* and *A. triphyllum*. Complementary sequences were rare across species. *A. flavum* and *A. ringens* exhibited unique patterns; with more reverse than forward sequences. *A. ringens* contained 48 reverse sequences compared to 37 forward sequences, while *A. flavum* had 30 reverse sequences versus 26 forward sequences. The distribution of palindromic sequences varied, with *A. erubescens* and *A. flavum* showing significant numbers (25 and 22, respectively), indicating a diverse sequence types within the plastomes (Table 2).

The MISA tool identified six classes of simple sequence repeats (SSRs), with total counts ranging from 126 in *A. ringens* to 224 copies in *A. bockii* (Table 3, Supplementary Table 3). Mononucleotides were the most abundant, comprising 73.02% in *A. ringens* (92 copies) to 37.5% in *A. bockii* (84 copies), followed by dinucleotides, which ranged from 24.11% in *A. bockii* (54 copies) to 8.73% in *A. ringens* (11 copies). Pentanucleotides and tetranucleotides ranked third and fourth in abundance. Pentanucleotides repeats varied from 16.17% in *A. nepenthoides* (25 copies) to 2.38% in *A. ringens* (3 copies); while tetranucleotides ranged from 13.77% in *A. nepenthoides* (26 copies) to 6.17% in *A. prazeri* (11 copies). Trinucleotides were the second least frequent, comprising 13.89% in *A. flavum* (20 copies) to 3.97% in *A. ringens* (5 copies). Hexanucleotides were the rarest, with *A. ringens* showing 3.17% (4 copies) and *A. bockii* only 0.89% (2 copies).

### Discussion

This study provides a high-resolution phylogenomic framework for *Arisaema* based on complete plastome sequences from 13 taxa (Fig. 2). Compared to prior studies relying on four chloroplast markers [38], our analysis offers greater confidence in phylogenetic placement, despite a smaller sample size. Notably, we observed discrepancies in the placement of *A. nepenthoides*, which our results position as a sister group to all other taxa rather than within clade IX. Further exploration, through expanded taxon sampling, morphological investigation, or additional genomic analyses, is needed to resolve its evolutionary placement.

The plastome of *Arisaema* taxa analyzed in this study range from 160,792 in *A. ringens* to 175,537 bp in *A. bockii*, maintaining the typical quadripartite structure found in angiosperm plastomes [41]. While gene content and organization remain largely conserved across species, specific structural variations were detected, such as the gene inversions observed in *A. prazeri*. This suggests that, despite extensive speciation since the Miocene epoch, the plastome structure of *Arisaema* has remained relatively stable. However, the limited representation of species in this study (11 out of



**Fig. 4** Alignment visualization of chloroplast genome sequences of 13 *Arisaema* taxa. VISTA-based identity plots display sequence conservation relative to the reference *Pinellia ternata*. The vertical scale represents sequence identity (50% to 100%). Gray arrows above the alignment indicate gene positions and orientations. Colors representing different genomic regions are shown in the legend at the bottom left

approximately 200 recognized taxa) necessitates caution in extrapolating these patterns to the entire genus.

Comparative analyses of IR-SC junctions further highlight plastomic variation within *Arisaema*. *A. nepenthoides* exhibited contracted IRs (25,130 bp), while *A. ringens* had the smallest LSC (88,915 bp) among sampled taxa. These variations align with patterns observed in other Araceae species, where IR contraction and expansion are often influenced by repeat sequences [13, 33]. Similar IR dynamics and gene rearrangements have been reported in other genera within the family, including *Pothos scandens*, *Anchomanes hookeri* and *Zantedeschia aethiopica* [1, 21].

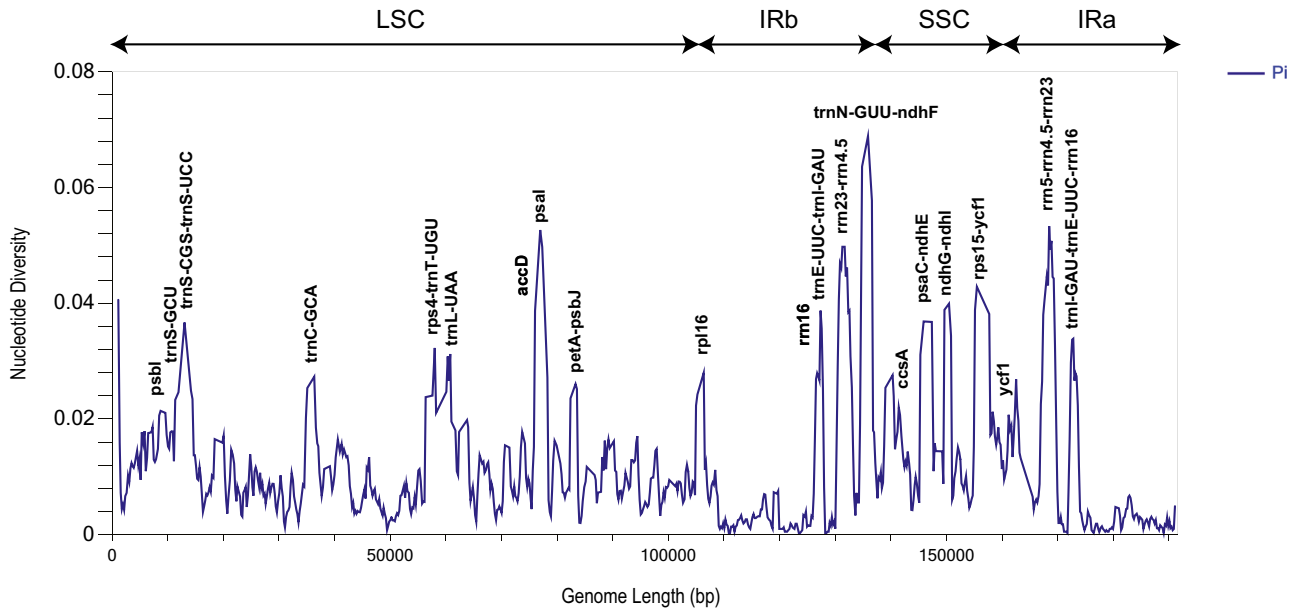


**Fig. 5** Genetic variation analysis across different genomic regions of *Arisaema* taxa using DnaSP

**Table 2** Distribution of sequence types (forward, reverse, complementary, and palindromic) in the plastomes of 13 *Arisaema* taxa

Taxa	Section	Type of sequences				
		Forward	Reverse	Complementary	Palindromic	
<i>A. prazeri</i> - China	This study	Odorata	41	32	6	11
<i>A. prazeri</i> - Thailand	MT884869	Odorata	41	32	6	11
<i>A. erubescens</i>	MT676834	Sinarisaema	30	27	8	25
<i>A. heterophyllum</i>	MZ424448	Flagellarisaema	42	27	7	14
<i>A. heterophyllum</i>	ON060885	Flagellarisaema	43	25	7	15
<i>A. bockii</i>	MZ380241	Pistillata	45	34	1	10
<i>A. nepenthoides</i>	MW338731	Nepenthoidea	45	20	6	19
<i>A. franchetianum</i>	SRR8655277	Franchetiana	37	34	2	17
<i>A. flavum</i>	MZ568767	Frimbiata	26	30	12	22
<i>A. decipiens</i>	ON360980	Decipientia	30	28	13	19
<i>A. triphyllum</i>	SRR18716441	Pedatisecta	41	24	7	18
<i>A. ringens</i>	MK111107	Pistillata	37	48	0	5
<i>A. amurensis</i>	OR789627	Pistillata	41	30	2	17

**Table 3** Classification and abundance of six simple sequence repeats (SSR) types in the plastomes of 13 *Arisaema* taxa

Taxa	Accession Number	Section	Repeat type classes					
			mono-	di-	tri-	tetra-	penta-	hexa-
<i>A. prazeri</i> - China	This study	Odorata	97	47	21	23	27	2
<i>A. prazeri</i> - Thailand	MT884869	Odorata	79	32	22	10	17	2
<i>A. erubescens</i>	MT676834	Sinarisaema	78	18	18	14	9	3
<i>A. heterophyllum</i>	MZ424448	Flagellarisaema	92	35	20	26	25	3
<i>A. heterophyllum</i>	ON060885	Flagellarisaema	91	34	19	26	25	3
<i>A. bockii</i>	MZ380241	Pistillata	84	54	25	27	32	2
<i>A. nepenthoides</i>	MW338731	Nepenthoidea	68	33	12	23	27	4
<i>A. franchetianum</i>	SRR8655277	Franchetiana	88	31	22	12	11	4
<i>A. flavum</i>	MZ568767	Frimbiata	79	20	20	14	8	3
<i>A. decipiens</i>	ON360980	Decipientia	83	33	18	15	18	4
<i>A. triphyllum</i>	SRR18716441	Pedatisecta	100	32	15	18	15	4
<i>A. ringens</i>	MK111107	Pistillata	92	11	5	11	3	4
<i>A. amurense</i>	OR789627	Pistillata	95	28	24	21	29	5

Further comparative analysis onto species from 13 genera in the subfamily Aroideae [22], four species from the tribe Monsteroideae [21], and the genus *Symplocarpus* [25] supports the notion that plastome architecture relatively conserved across closely related taxa.

Structural conservation within *Arisaema* plastomes was also evident in Mauve alignment results, which revealed syntenic blocks across taxa. The inversion of specific blocks in *A. prazeri* suggests possible recombination events or selective pressures influencing plastome evolution [11]. The distinct organization of *A. triphyllum* hints at deviations from the typical plastome structure observed in the genus. These findings underscore the balance between conservation and variation in plastome evolution, where localized genomic changes may contribute to species adaptation while maintaining core structural stability.

mVISTA analysis demonstrated that the LSC region exhibits the highest sequences divergence among *Arisaema* species, with the IR regions being the most conserved. This pattern is consistent with observations in *Symplocarpus* [25] and duckweeds (Lemnoideae) [13].

The repeat structures analysis underscores the genomic complexity within *Arisaema*. Forward sequences were the most abundant, while palindromic sequences varied among taxa, with *A. erubescens* and *A. flavum* displaying the highest counts. SSR analysis revealed that mononucleotides were the predominant repeat type, with *A. bockii* containing the highest SSR count (224) and *A. ringens* the lowest (126). Notably, *A. flavum* and *A. ringens* exhibited an unusual abundance of reverse sequences, warranting further investigation into their potential evolutionary significance. Variability in repeat structures may play a role in IR contraction and expansion, contributing to plastome evolution [46].

The nucleotide diversity analysis highlighted significant genetic variation within *Arisaema*, with a haplotype diversity (Hd) of 1.000 and moderate nucleotide diversity ( $\pi=0.01059$ ). Sliding window analysis identified regions of elevated diversity, particularly within the SSC (*trnH-GUG*, *trnN-GUU*, and *ndhF*;  $\pi=0.06887$ ) and *ycf1* ( $\pi=0.03882$ ), suggesting these loci may be under selective pressures. Conversely, highly conserved regions, such as those at the genome's terminal ends ( $\pi$  as low as 0.00026), likely represent functionally essential elements [42]. High-diversity regions may serve as valuable phylogenetic markers, while conserved sequences offer potential for taxonomic classification [14].

Despite the rapid morphological diversification of *Arisaema*, our findings suggest that plastome structure remains relatively stable across species. This indicates that plastome evolution may be decoupled from morphological changes. However, structural variations such as gene inversions, repeat elements, and indels provide insights into genetic differentiation and potential adaptation [15]. Future studies incorporating nuclear and mitochondrial genomes will be crucial for understanding the broader evolutionary dynamics shaping *Arisaema* diversification.

Given the limited genomic resources available for *Arisaema*, expanding efforts in transcriptomic and functional genomic studies will be essential. Such approaches will help link plastome features to adaptive traits, ultimately enhancing our understanding of the evolutionary and ecological dynamics of this diverse genus.

**Supplementary Information** The online version contains supplementary material available at <https://doi.org/10.1007/s13237-025-00554-1>.

**Acknowledgements** Computational resources were provided by the e-INFRA CZ project (ID: 90254), supported by the Ministry of Education, Youth and Sports of the Czech Republic.

**Author contributions** All authors contributed to the study conception and design. Material preparation, and data collection were performed by SL. Data analysis was performed by SLL. The first draft of the manuscript was written by SLL; and SL revised the manuscript. All authors read and approved the final manuscript.

**Funding** No funding was received for conducting this study.

## Declarations

**Conflict of interest** The authors declare no conflict of interest.

## References

- Abdullah, Henrique CL, Mehmood F, Carlsen MM, Islam M, Waheed MT, Poczai P, Croat TB, Ahmed I. Complete chloroplast genomes of *Anthurium huixtlense* and *Pothos scandens* (Pothoideae, Araceae): unique inverted repeat expansion and contraction affect rate of evolution. *J Mol Evol.* 2020;88:562–74.
- Amiryousefi A, Hyvönen J, Poczai P. IRscope: an online program to visualize the junction sites of chloroplast genomes. *Bioinformatics.* 2018;34:3030–1.
- Andrews S. FastQC: a quality control tool for high throughput sequence data. (2010). Available online at: <http://www.bioinformatics.babraham.ac.uk/projects/fastqc>.
- Bankevich A, Nurk S, Antipov D, Gurevich AA, Dvorkin M, Kulikov AS, Lesin VM, Nikolenko SI, Pham S, Prjibelski AD, Pyshkin AV, Sirotkin AV, Vyahhi N, Tesler G, Alekseyev MA, Pevzner PA. SPAdes: a new genome assembly algorithm and its applications to single-cell sequencing. *J Comput Biol.* 2012;19:455–77.
- Beier S, Thiel T, Münch T, Scholz U, Mascher M. MISA-web: a web server for microsatellite prediction. *Bioinformatics.* 2017;33:2583–5.
- Cai XL, Wang JH, Zhao KK, Wang HX, Zhu ZX, Wang HF. Complete plastome sequence of *Arisaema ringens* (Araceae): a dioecious herb disjunctly distributed in China, Japan and Korea. *Mitochondrial DNA Part B.* 2019;4:540–1.
- Charboneau JLM, Cronn RC, Liston A, Wojciechowski MF, Sanderson MJ. Plastome structural evolution and homoplastic inversions in Neo-Astragalus (Fabaceae). *Genome Biol Evol.* 2021;13:eva2b15.
- Choi IS, Jansen R, Ruhlman T. Lost and found: return of the inverted repeat in the legume clade defined by its absence. *Genome Biol Evol.* 2019;11:1321–33.
- Croat T. Ecology and life forms of Araceae. *Aroideana.* 1988;11:4–52.
- Darling ACE, Mau B, Blattner FR, Perna NT. Mauve: multiple alignment of conserved genomic sequence with rearrangements. *Genome Res.* 2004;14:1394–403.
- Darling AE, Mau B, Perna NT. ProgressiveMauve: multiple genome alignment with gene gain, loss and rearrangement. *PLoS ONE.* 2010;5(6):e11147.
- Díez Menéndez C, Poczai P, Williams B, Myllys L, Amiryousefi A. IRplus: an augmented tool to detect inverted repeats in plastid genomes. *Genome Biol Evol.* 2023;15:evad177.
- Ding Y, Fang Y, Guo L, Li Z, He K, Zhao Y, Zhao H. Phylogenetic study of Lemnoideae (duckweeds) through complete chloroplast genomes for eight accessions. *PeerJ.* 2017;5:e4186.
- Dong W, Liu J, Yu J, Wang L, Zhou S. Highly variable chloroplast markers for evaluating plant phylogeny at low taxonomic levels and for DNA barcoding. *PLoS ONE.* 2012;7(4):e35071.
- Feulner PGD, De-Kayne R. Genome evolution, structural rearrangements and speciation. *J Evol Biol.* 2017;30(8):1488–90.
- Frailely DC, Chaluvadi SR, Vaughn JN, et al. Gene loss and genome rearrangement in the plastids of five Hemiparasites in the family Orobanchaceae. *BMC Plant Biol.* 2018;18:30.
- Frazer KA, Pachter L, Poliakov A, Rubin EM, Dubchak I. VISTA: computational tools for comparative genomics. *Nucleic Acids Res.* 2004;32:W273–9.
- Govaerts R, Bogner J, Boos J, Boyce P, Cosgriff B, Croat T, Goncalves E, Grayum M, Hay A, Hettterscheid W, Ittenbach S, Landolt E, Mayo S, Murata J, Nguyen VD, Sakuragui CM, Singh Y, Thompson S, Zhu G. World checklist of Araceae [online]. Available from <http://apps.kew.org/wcsp/> [Accessed 1 May 2024] (2019)
- Gruzdev EV, Kadnikov VV, Beletsky AV, Mardanov AV, Ravin NV. Extensive plastome reduction and loss of photosynthesis genes in *Diphelypaea coccinea*, a holoparasitic plant of the family Orobanchaceae. *PeerJ.* 2019;7:e7830.
- Gusman G, Gusman L. The genus *Arisaema*—a monograph for botanists and nature lovers, Second revised and enlarged edition. A.R.G. Gantner Verlag, Ruggell. (2006)
- Henrique CL, Abdullah AI, Carlsen MM, Zuluaga A, Croat TB, McKain MR. Molecular evolution of chloroplast genomes in Monsteroideae (Araceae). *Planta.* 2020;251:72.
- Henriquez CL, Abdullah AI, Carlsen MM, Zuluaga A, Croat TB, McKain MR. Evolutionary dynamics in chloroplast genome of subfamily Aroideae (Araceae). *Genomics.* 2020;112:2349–60.
- Jin JJ, Yu WB, Yang JB, Song Y, dePamphilis CW, Yi TS, Li DZ. GetOrganelle: a fast and versatile toolkit for accurate de novo assembly of organelle genomes. *Genome Biol.* 2020;21:241.
- Katoh K, Standley DM. MAFFT multiple sequence alignment software version 7: improvements in performance and usability. *Mol Biol Evol.* 2013;30:772–80.
- Kim SH, Yang JY, Park J, Yamada T, Maki M, Kim SC. Comparison of whole plastome sequences between thermogenic skunk cabbage *Symplocarpus renifolius* and nonthermogenic *S. nipponicus* (Orontioideae; Araceae) in East Asia. *Int J Mol Sci.* 2019;20:4678.
- Kim W, Lautenschläger T, Bolin JF, et al. Extreme plastomes in holoparasitic Balanophoraceae are not the norm. *BMC Genomics.* 2023;24:330.
- Köhler M, Reginato M, Jin JJ, Majure LC. More than a spiny morphology: plastome variation in the prickly pear cacti (Opuntieae). *Ann Bot.* 2023;132:771–86.
- Kurtz S, Choudhuri JV, Ohlebusch E, Schleiermacher C, Stoye J, Giegerich R. REPuter: the manifold applications of repeat analysis on a genomic scale. *Nucleic Acids Res.* 2001;29:4633–42.
- Langmead B, Salzberg SL. Fast gapped-read alignment with Bowtie. *Nat Methods.* 2012;9:357–9.
- Low SL, Yu C-C, Ooi IH, Eiadthong W, Galloway A, Zhou Z-K, Xing Y-W. Extensive Miocene speciation in and out of Indochina: the biogeographic history of *Typhonium sensu stricto* (Araceae) and its implication for the assembly of Indochina flora. *J Syst Evol.* 2021;59:419–28.
- Ma ZX, Li H. The genus *Arisaema* (Araceae: Aroideae: Arisaemateae) in China—a taxonomic revision and annotated list of species. *Aroideana.* 2017;40:49–134.
- Manudev KM, Arunkumar PG, Nampy S. Taxonomic revision of *Arisaema* sect. *Sinarisaema* in India. *Rheedea.* 2019;29:119–73.
- Mardanov AV, Ranin NV, Kuznestsov BB, Samigullin TH, Antonov AS, Kolganova TV, Skyabin KG. Complete sequence of the Duckweed (*Lemna minor*) chloroplast genome: structural organization and phylogenetic relationships to other Angiosperms. *J Mol Evol.* 2008;66:555–64.
- Minh BQ, Schmidt HA, Chernomor O, Schrempf D, Woodhams MD, von Haeseler A, Lanfear R. IQ-TREE 2: new models and

- efficient methods for phylogenetic inference in the genomic era. *Mol Biol Evol.* 2020;37:1530–4.
35. Murata J. *Arisaema* in Japan—the picture book of plant systematics in color. Tokyo: Hokuryukan Publishing Co., Ltd.; 2011.
  36. Murata J, Wu S, Sasamura K, Ohi-Toma T. Comments on the taxonomic treatment of *Arisaema* (Araceae) in flora of China. *Acta Phytotaxon Geobot.* 2014;65:161–76.
  37. Nauheimer L, Metzler D, Renner SS. Global history of the ancient monocot family Araceae inferred with models accounting for past continental positions and previous ranges based on fossils. *New Phytol.* 2012;195:938–50.
  38. Ohi-Toma T, Wu S, Murata H, Murata J. An updated genus-wide phylogenetic analysis of *Arisaema* (Araceae) with reference to sections. *Bot J Linn Soc.* 2016;182:100–14.
  39. Rozas J, Ferrer-Mata A, Sánchez-DelBarrio JC, Guirao-Rico S, Librado P, Ramos-Onsins SE, Sánchez-Gracia A. DnaSP 6: DNA sequence polymorphism analysis of large data sets. *Mol Biol Evol.* 2017;34:3299–302.
  40. Ruhlman TA, Jansen RK. Plastid genomes of flowering plants: essential principles. In: Maliga P, editor. *Chloroplast biotechnology: methods and protocols, methods in molecular biology.* US, New York: Springer; 2021. p. 3–47.
  41. Shinozaki K, Ohme M, Tanaka M, Wakasugi T, Hayashida N, Matsubayashi T, et al. The complete nucleotide sequence of the tobacco chloroplast genome: its gene organization and expression. *Eur Mol Biol Org J.* 1986;5:2043–9.
  42. Sukhrmani G, Maurya S, Choudhary RK. Plastome comparison reveals hotspots of nucleotide diversity and positive selection pressure on *accD*, *matK*, *psaA* and *rbcL* genes in Smilacaceae. *Braz J Bot.* 2024;47:145–61.
  43. Thiel T, Michalek W, Varshney R, Graner A. Exploiting EST databases for the development and characterization of gene-derived SSR-markers in barley (*Hordeum vulgare* L.). *Theor Appl Genet.* 2003;106:411–22.
  44. Tillich M, Lehwark P, Pellizzer T, Ulbricht-Jones ES, Fischer A, Bock R, Greiner S. GeSeq—versatile and accurate annotation of organelle genomes. *Nucleic Acids Res.* 2017;45:W6–11.
  45. Vera-Paz SI, Díaz DDDC, Jost M, Wanke S, Rossado AJ, Hernández-Gutiérrez R, Salazar GA, Magallón S, Gouda EJ, Ramírez-Morillo IM, Donadio S, Mendoza CG. New plastome structural rearrangements discovered in core Tillandsioideae (Bromeliaceae) support recently adopted taxonomy. *Front Plant Sci.* 2022;13:924922.
  46. Wu S, Chen J, Li Y, Liu A, Li A, Yin M, Shrestha N, Liu J, Ren G. Extensive genomic rearrangements mediated by repetitive sequences in plastomes of *Medicago* and its relatives. *BMC Plant Biol.* 2021;21:421.
  47. Zhang Y, Guo X, Yan B. Characterization of the complete chloroplast genome of *Arisaema erubescens* (Wall.) Schott, a traditional Chinese medicinal herb. *Mitochondrial DNA Part B.* 2020;5(3):3149–50.
- Publisher's Note** Springer Nature remains neutral with regard to jurisdictional claims in published maps and institutional affiliations.
- Springer Nature or its licensor (e.g. a society or other partner) holds exclusive rights to this article under a publishing agreement with the author(s) or other rightsholder(s); author self-archiving of the accepted manuscript version of this article is solely governed by the terms of such publishing agreement and applicable law.